



XXVIIth International Conference on Ultrarelativistic Nucleus-Nucleus Collisions
(Quark Matter 2018)

Electroweak boson measurements in p-Pb and Pb-Pb collisions at $\sqrt{s_{NN}} = 5.02$ TeV with ALICE at the LHC

Mohamad Tarhini
for the ALICE Collaboration

SUBATECH, IMT Atlantique, Université de Nantes, CNRS-IN2P3, Nantes, France

Abstract

The ALICE collaboration has measured the electroweak boson production at forward rapidity in Pb-Pb and p-Pb collisions at $\sqrt{s_{NN}} = 5.02$ TeV. Final results on the Z^0 boson production in Pb-Pb collisions are presented as a function of centrality and rapidity. Calculations based on free parton distribution functions overestimate the measurement up to 3σ . In addition, final results on W^\pm and Z^0 bosons production in p-Pb collisions at the same energy will be presented and discussed.

Keywords: Heavy ion collisions, electroweak bosons, ALICE.

1. Introduction

The measurement of electroweak bosons (W^\pm and Z^0) has become possible for the first time in heavy ion collisions at the LHC [1–8] thanks to the large collision energies and luminosities. Electroweak bosons are created in the hard scattering processes at the initial stage of the collision, and they are unaffected by the presence of the strongly interacting medium. This makes them clean probes of the initial state effects in heavy ion collisions, such as the nuclear modification of the Parton Distribution Functions (PDFs). The different sets that parametrize this modification suffer currently from large uncertainties due to the lack of experimental data used to constrain their models. The measurements of W^\pm and Z^0 bosons is accessible over a large range of rapidity by the different LHC experiments giving an access to a region of high virtuality ($Q^2 \sim M_{W,Z}^2$) and a wide range of Bjorken- x values (from about 10^{-4} to almost unity) in which the nuclear PDFs (nPDFs) are poorly constrained from previous experiments [9].

2. Analysis and results

A detailed description of the ALICE detector can be found in [10]. W^\pm and Z^0 bosons are reconstructed via their muon and dimuon decay channels respectively, using the forward muon spectrometer that covers the pseudorapidity range $-4 < \eta < -2.5$. In p-Pb collisions at $\sqrt{s_{NN}} = 5.02$ TeV, the p (Pb) beam going

towards the muon spectrometer allows us to access the forward (backward) center-of-mass rapidity region $2.03 < y_{\text{cms}} < 3.53$ ($-4.46 < y_{\text{cms}} < -2.96$). Both the beam configurations, p-going and Pb-going directions, were analyzed. The integrated luminosities collected in these two periods are respectively $5.03 \pm 0.18 \text{ nb}^{-1}$ and $5.81 \pm 0.20 \text{ nb}^{-1}$. In Pb-Pb collisions at $\sqrt{s_{\text{NN}}} = 5.02 \text{ TeV}$, the analysis was performed using an integrated luminosity of $\sim 225 \mu\text{b}^{-1}$, the centrality was estimated by fitting the V0 detector amplitude using an MC Glauber [11] to extract the number of binary collisions, N_{coll} , and of participating nucleons, N_{part} . The W^\pm boson candidates are extracted from a Monte Carlo (MC) template fit of the transverse momentum distribution of single muons. Concerning the Z^0 boson, the selection of muon tracks (pseudorapidity $-4 < \eta^\mu < -2.5$ and transverse momentum $p_{\text{T}}^\mu > 20 \text{ GeV}/c$) left a nearly background-free sample, and the signal is extracted by counting the entries in the invariant-mass distribution of opposite-sign muon pairs in the region $60 < M_{\mu\mu} < 120 \text{ GeV}/c^2$. More details on the analysis strategy can be found in [2].

2.1. p-Pb collisions

The rapidity differential cross-section of the Z^0 boson production in the dimuon decay channel with $p_{\text{T}} > 20 \text{ GeV}/c$ is shown in the left panel of Fig. 1. The middle and right panels show the cross-section for muons with $p_{\text{T}} > 10 \text{ GeV}/c$ from W^- and W^+ boson production, respectively. For both W^\pm and Z^0 bosons, the results are compared to NLO and NNLO theoretical calculations with and without including the nuclear modification of the PDFs. Both calculations from [9] at NLO using the CT10 [12] PDF set (blue hatched boxes), as well as NNLO calculations based on FEWZ [13] with the MSTW2008 [14] PDF set (blue filled boxes) are able to describe the data within uncertainties. The results are also compared to the corresponding calculations including the EPS09 NLO [15] parametrization of the nuclear modification of the PDFs (hatched and filled red boxes respectively). The inclusion of the nuclear effects results in a slight reduction of the cross-section. However, this reduction is smaller than the experimental uncertainties which prevents a discrimination between the different calculations.

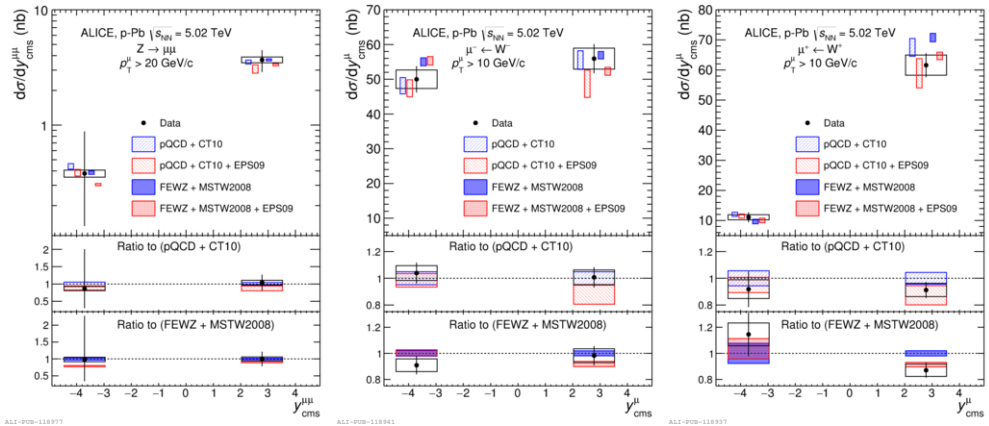


Fig. 1. Rapidity-differential cross section of Z^0 (left panel), W^- (middle panel) and W^+ (right panel) boson production in p-Pb collisions at $\sqrt{s_{\text{NN}}} = 5.02 \text{ TeV}$. The vertical bars (boxes) are the statistical (systematic) uncertainties. Results are compared with NLO [9] and NNLO calculations [13] with and without including the nuclear modification of the PDFs. In the top panel, the calculations are shifted in rapidity for a better visibility. The vertical middle (bottom) panel shows the ratio of data and NLO (NNLO) calculations divided by the NLO (NNLO) calculations without including nuclear modification of the PDFs.

2.2. Pb-Pb collisions

The Z^0 boson invariant yield normalized to the average nuclear overlap function $\langle T_{AA} \rangle$ is shown in Fig. 2 for 0–90% centrality and integrated in rapidity ($2.5 < y < 4.0$). The comparison with theoretical calculations

at NLO is shown. The CT14 [16] calculation utilises free proton and neutron PDFs taking into account the isospin effects of the Pb nucleus. This calculation overestimates the measurement by 2.3σ . The other three calculations include nuclear modifications of the PDFs using three different parametrizations (EPPS16 [17], EPS09 [15], and nCTEQ15 [18, 19]) and they are in agreement with the measurement within uncertainties.

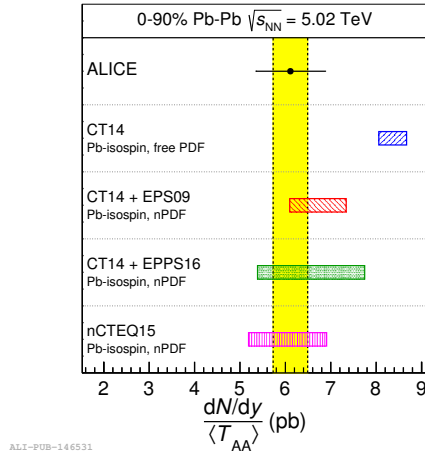


Fig. 2. Z^0 boson invariant yield in $2.5 < y < 4.0$ divided by the average nuclear overlap function for 0–90% centrality. The horizontal solid line represents the statistical uncertainty of the measurement while the yellow filled band shows the systematic uncertainty. The result is compared to theoretical calculations with and without including nuclear modification of the PDFs [15–19].

The rapidity dependence of the Z^0 boson invariant yields divided by $\langle T_{AA} \rangle$ is shown in the left panel of Fig. 3. The results are compared to pQCD calculations using the CT14 [16] PDF set both with (green filled box) and without (blue hatched box) including nuclear modifications of the PDFs using the EPPS16 [17] parameterization. The calculations based on vacuum PDFs overestimate the measurement in the two rapidity intervals, whereas those that include nuclear modifications are in good agreement with data. The right panel of Fig. 3 shows the Z^0 boson invariant yields divided by $\langle T_{AA} \rangle$ as a function of the collision centrality expressed in terms of the number of participants weighted by the number of binary collisions ($\langle N_{part} \rangle_{N_{coll}}$). The results are compared to calculations including a centrality-dependent nuclear modification of the PDFs [20], which describe the data within uncertainties.

3. Conclusions

The ALICE experiment studied the W^\pm and Z^0 bosons production at backward and forward rapidity in p-Pb collisions at $\sqrt{s_{NN}} = 5.02$ TeV [2]. The measured cross sections are compatible within uncertainties with NLO and NNLO calculations with and without including the nuclear modifications of the PDFs. Better precision is required in order to discriminate between the different calculations. The Z^0 boson production was also studied at forward rapidity in Pb-Pb collisions at $\sqrt{s_{NN}} = 5.02$ TeV [1]. Calculations that include nuclear modification of the PDFs are in agreement with the measurement within uncertainty. In contrast, calculations with vacuum PDFs overestimate the centrality-integrated Z^0 boson invariant yield by 2.3σ .

References

- [1] ALICE Collaboration, S. Acharya, et al., Measurement of Z^0 -boson production at large rapidities in Pb-Pb collisions at $\sqrt{s_{NN}} = 5.02$ TeV, Phys. Lett. B780 (2018) 372–383. arXiv:1711.10753, doi:10.1016/j.physletb.2018.03.010.
- [2] ALICE Collaboration, J. Adam, et al., W and Z boson production in p-Pb collisions at $\sqrt{s_{NN}} = 5.02$ TeV, JHEP 02 (2017) 077. arXiv:1611.03002, doi:10.1007/JHEP02(2017)077.

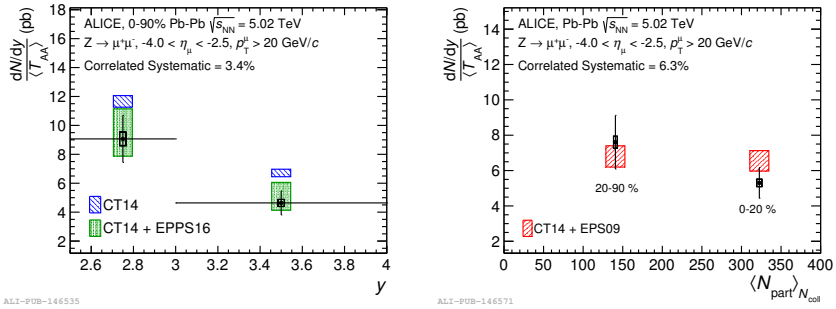


Fig. 3. Left (Right): rapidity (centrality) dependence of the Z^0 boson invariant yield divided by the average nuclear overlap function. The vertical error bars are statistical only, while the open boxes represent the systematic uncertainties. The rapidity dependence results are compared to theoretical calculations with [16] and without [17] nuclear modification of the PDFs. The centrality dependence results are compared to theoretical calculations with centrality-dependent nPDFs [15, 20].

- [3] ATLAS Collaboration, G. Aad, et al., Measurement of Z boson Production in Pb+Pb Collisions at $\sqrt{s_{NN}} = 2.76$ TeV with the ATLAS Detector, *Phys.Rev.Lett.* 110 (2) (2013) 022301. arXiv:1210.6486, doi:10.1103/PhysRevLett.110.022301.
- [4] ATLAS Collaboration, G. Aad, et al., Z boson production in p +Pb collisions at $\sqrt{s_{NN}} = 5.02$ TeV measured with the ATLAS detector, *Phys. Rev. C* 92 (4) (2015) 044915. arXiv:1507.06232, doi:10.1103/PhysRevC.92.044915.
- [5] LHCb Collaboration, R. Aaij, et al., Observation of Z production in proton-lead collisions at LHCb, *JHEP* 1409 (2014) 030. arXiv:1406.2885, doi:10.1007/JHEP09(2014)030.
- [6] CMS Collaboration, S. Chatrchyan, et al., Study of W boson production in PbPb and pp collisions at $\sqrt{s_{NN}} = 2.76$ TeV, *Phys.Lett.* B715 (2012) 66–87. arXiv:1205.6334, doi:10.1016/j.physletb.2012.07.025.
- [7] CMS Collaboration, S. Chatrchyan, et al., Study of Z production in PbPb and pp collisions at $\sqrt{s_{NN}} = 2.76$ TeV in the dimuon and dielectron decay channels, *JHEP* 1503 (2015) 022. arXiv:1410.4825, doi:10.1007/JHEP03(2015)022.
- [8] CMS Collaboration, V. Khachatryan, et al., Study of Z boson production in pPb collisions at $\sqrt{s_{NN}} = 5.02$ TeV, *Phys. Lett.* B759 (2016) 36–57. arXiv:1512.06461, doi:10.1016/j.physletb.2016.05.044.
- [9] H. Paukkunen, C. A. Salgado, Constraints for the nuclear parton distributions from Z and W production at the LHC, *JHEP* 03 (2011) 071. arXiv:1010.5392, doi:10.1007/JHEP03(2011)071.
- [10] ALICE Collaboration, K. Aamodt, et al., *JINST* 3 (2008) S08002. doi:10.1088/1748-0221/3/08/S08002.
- [11] ALICE Collaboration Collaboration, J. Adam, et al., *Phys. Rev. Lett.* 116 (2016) 222302.
- [12] H.-L. Lai, M. Guzzi, J. Huston, Z. Li, P. M. Nadolsky, J. Pumplin, C. P. Yuan, New parton distributions for collider physics, *Phys. Rev. D* 82 (2010) 074024. arXiv:1007.2241, doi:10.1103/PhysRevD.82.074024.
- [13] R. Gavin, Y. Li, F. Petriello, S. Quackenbush, FEWZ 2.0: A code for hadronic Z production at Next-to-Next-to-Leading order, *Comput. Phys. Commun.* 182 (2011) 2388–2403. arXiv:1011.3540, doi:10.1016/j.cpc.2011.06.008.
- [14] A. D. Martin, W. J. Stirling, R. S. Thorne, G. Watt, Parton distributions for the LHC, *Eur. Phys. J.* C63 (2009) 189–285. arXiv:0901.0002, doi:10.1140/epjc/s10052-009-1072-5.
- [15] K. J. Eskola, H. Paukkunen, C. A. Salgado, EPS09: A New Generation of NLO and LO Nuclear Parton Distribution Functions, *JHEP* 04 (2009) 065. arXiv:0902.4154, doi:10.1088/1126-6708/2009/04/065.
- [16] S. Dulat, T.-J. Hou, J. Gao, M. Guzzi, J. Huston, P. Nadolsky, J. Pumplin, C. Schmidt, D. Stump, C. P. Yuan, New parton distribution functions from a global analysis of quantum chromodynamics, *Phys. Rev. D* 93 (2016) 033006. arXiv:1506.07443, doi:10.1103/PhysRevD.93.033006.
- [17] K. J. Eskola, P. Paakkinen, H. Paukkunen, C. A. Salgado, EPPS16: Nuclear parton distributions with LHC data, *Eur. Phys. J.* C77 (2017) 163. arXiv:1612.05741, doi:10.1140/epjc/s10052-017-4725-9.
- [18] K. Kovarik, et al., nCTEQ15 - Global analysis of nuclear parton distributions with uncertainties in the CTEQ framework, *Phys. Rev. D* 93 (2016) 085037. arXiv:1509.00792, doi:10.1103/PhysRevD.93.085037.
- [19] A. Kusina, F. Lyonnet, D. B. Clark, E. Godat, T. Jezo, K. Kovarik, F. I. Olness, I. Schienbein, J. Y. Yu, Vector boson production in proton-lead and lead-lead collisions at the LHC and its impact on nCTEQ15 PDFs arXiv:1610.02925.
- [20] I. Helenius, K. J. Eskola, H. Honkanen, C. A. Salgado, Impact-Parameter Dependent Nuclear Parton Distribution Functions: EPS09s and EKS98s and Their Applications in Nuclear Hard Processes, *JHEP* 07 (2012) 073. arXiv:1205.5359, doi:10.1007/JHEP07(2012)073.